Available online at www.sciencedirect.com
SCIENCE DIRECT®
Journal of Nuclear Materials 348 (2006) 223–227
journal of nuclear materials
www.elsevier.com/locate/jnucmat

Letter to the Editors

Phase transformation induced by ion implantation in cubic stabilized zirconia

G. Sattonnay [a,*], L. Thomé [b]

[a] Laboratoire d'Etudes des Matériaux Hors Equilibre, ICMMO, CNRS UMR 8647, Université Paris Sud, Bât. 410, F-91405 Orsay campus, France
[b] Centre de Spectrométrie Nucléaire et de Spectrométrie de Masse, IN2P3-CNRS, Université Paris Sud, Bât. 104-108, F-91405 Orsay campus, France

Received 29 March 2005; accepted 2 September 2005

Abstract

Cubic yttria-stabilized zirconia possesses a high stability against radiation. No amorphization of this material has been observed, even at high ion fluences leading to the production of a large amount of defects. Nevertheless irradiation with energetic particles may induce microstructural evolutions and phase transformations. In the present paper we demonstrate that a cubic-to-rhombohedral phase transformation occurs in yttria-stabilized zirconia implanted with He ions. This transformation consists in a rhombohedral deformation of the cubic cell along the ⟨1 1 1⟩ directions due to residual stresses induced by implantation.

1. Introduction

Cubic stabilized zirconia is one of the most promising materials for use as inert matrix for actinide transmutation or immobilization [1]. These applications are based on refractory properties, high chemical durability, ability to incorporate actinides and excellent radiation stability. Pure zirconia has three polymorphic phases, with the following phase transitions [2]:

$$\text{monoclinic (m)} \xrightarrow{1170\,^{\circ}\text{C}} \text{tetragonal (t)} \xrightarrow{2370\,^{\circ}\text{C}} \text{cubic (c)} \xrightarrow{2680\,^{\circ}\text{C}} \text{liquid.}$$

The cubic phase has the fluorite-type structure (CaF_2). The high-temperature phases can be stabilized down to room temperature by doping pure zirconia with other oxides such as Y_2O_3, CaO or MgO [3]. In the case where the doping species is yttria, the cubic phase is stabilized at room temperature from a concentration of 8 mol% Y_2O_3.

Nuclear fuel matrices are submitted to severe radiative environment which can induce structural and microstructural evolutions leading to a modification of the material properties. In pure zirconia, a monoclinic-to-tetragonal phase transition was observed under ion irradiation [4–9]. The displacive

* Corresponding author. Tel.: +33 1 69 15 70 37; fax: +33 1 69 15 48 19.
E-mail address: gael.sattonnay@lemhe.u-psud.fr (G. Sattonnay).

0022-3115/$ - see front matter © 2005 Elsevier B.V. All rights reserved.
doi:10.1016/j.jnucmat.2005.09.005

character of this phase transformation was particularly investigated within the Landau theory approach [10].

The present paper reports a new phase transformation induced by He ion implantation in cubic yttria-stabilized zirconia (CYSZ) which might affect the physico-chemical properties of the material when used as actinide-bearing matrix.

2. Experimental procedures

Cubic zirconia polycrystals with 10 mol% Y_2O_3 were supplied by the Saint-Gobain-Desmarquest company. The specimens were polished with a 1 μm diamond paste to an optical finishing and were then annealed at 1400 °C for 10 h with a slow cooling down rate. Annealed samples were implanted with 120 keV He^+ ions at room temperature at the IRMA facility of the CSNSM in Orsay. Various fluences from 10^{15} up to 5×10^{16} cm^{-2} were used, which corresponds to He concentrations from 0.05 up to 2.7 at.% respectively. The Monte-Carlo SRIM2003 code [11] provides a value of the He-ion projected range (R_p) of 410 nm with a range straggling (ΔR_p) of 110 nm.

Irradiated samples were analyzed by grazing-incidence X-ray diffraction (GXRD) using a X'pert Pro MRD PANalytical diffractometer with the Cu K_α radiation and an angle of incidence of 2° to probe the implanted layer. X-ray patterns were recorded from 27° to 130° (2θ) with steps of 0.02°; the acquisition time was 10 s per step. In addition, residual stresses were determined by GXRD using the $\sin^2\Psi$ method [12]; the (3 3 1) peak of cubic zirconia was selected and recorded for several values of Ψ between −50° and +50°.

3. Results and discussion

Fig. 1(a) presents GXRD patterns recorded on zirconia polycrystals before and after He implantation at a fluence of 5×10^{16} cm^{-2}. Only the diffraction peaks corresponding to the cubic structure are exhibited on the unimplanted sample. A new diffraction line appears in the low-angle side of every diffraction peaks in the case of the He-implanted sample. A zoom of the 58–64° angular range presented in the inset of Fig. 1(a) clearly shows the presence of an additional peak. Fig. 1(b) shows a comparison between experimental GXRD data on He-implanted sample and the pattern calculated by LeBail fitting.

Analysis of the diffraction patterns with PowderV2 [13] and the GSAS package [14] indicates that the new diffraction peaks may be attributed to the formation of a rhombohedral phase. The cubic-to-rhombohedral (c → r) phase transformation consists in a rhombohedral deformation of the YSZ cubic cell along the ⟨1 1 1⟩ directions. Using the whole pattern LeBail fitting, following values of the rhombohedral lattice parameters are obtained for the highest fluence used (5×10^{16} cm^{-2}): $a = 0.36670(9)$ nm and $\alpha = 59.7°$ ($Z = 1$) or $a_H = 0.36526(2)$ and $c_H = 0.89998(9)$ nm ($Z = 3$) in the equivalent triple hexagonal cell; the rhombohedral cell vol-ume is 0.1040 nm^3. As a comparison, the cubic zirconia phase before implantation has a parameter $a = 0.51400(2)$ nm, which gives a volume of 0.1018 nm^3 for the primitive rhombohedral cell. Thus, the volume of the rhombohedral cell produced by He implantation is larger by about 2.2% than that of the primitive rhombohedral cell of unimplanted sample. Furthermore, after implantation the remaining cubic phase has a cell parameter which increases between 0.51442(2) and 0.51481(2) nm with increasing ion fluence. Fig. 2 shows that the c → r phase transformation is exhibited for the samples implanted at 5×10^{15}, 10^{16} and 5×10^{16} cm^{-2} (but not at 10^{15} cm^{-2}). The area of the diffraction peaks due to the new phase increases with increasing fluence from a few 10^{15} up to 10^{16} cm^{-2}, and then decreases slightly at 5×10^{16} cm^{-2}.

The macroscopic strain and the residual stress sensed by the cubic cell were also estimated by the $\sin^2\Psi$ method (Fig. 3). No stress is found in the unimplanted sample. A compressive stress is obtained in the cubic phase of the implanted layer. This stress is already observed at 10^{15} cm^{-2} and it increases with increasing fluence up to a saturation value of −700 MPa at 10^{16} cm^{-2}.

The presence of both He atoms and radiation damage leads to a volume expansion of the host lattice in the surface region of implanted samples. Moreover, some helium bubbles could also be formed at room temperature at the highest fluences. Since this volume expansion does not occur in the underlying undamaged region of the material, a lateral (i.e. perpendicular to the normal to the surface of the sample) residual stress is created. Thus, a compressive stress occurs in the implanted surface layer and a tensile stress takes place in the undamaged deeper layer. The occurrence of this compressive stress could be the cause of the c → r phase transformation observed in the implanted layer.

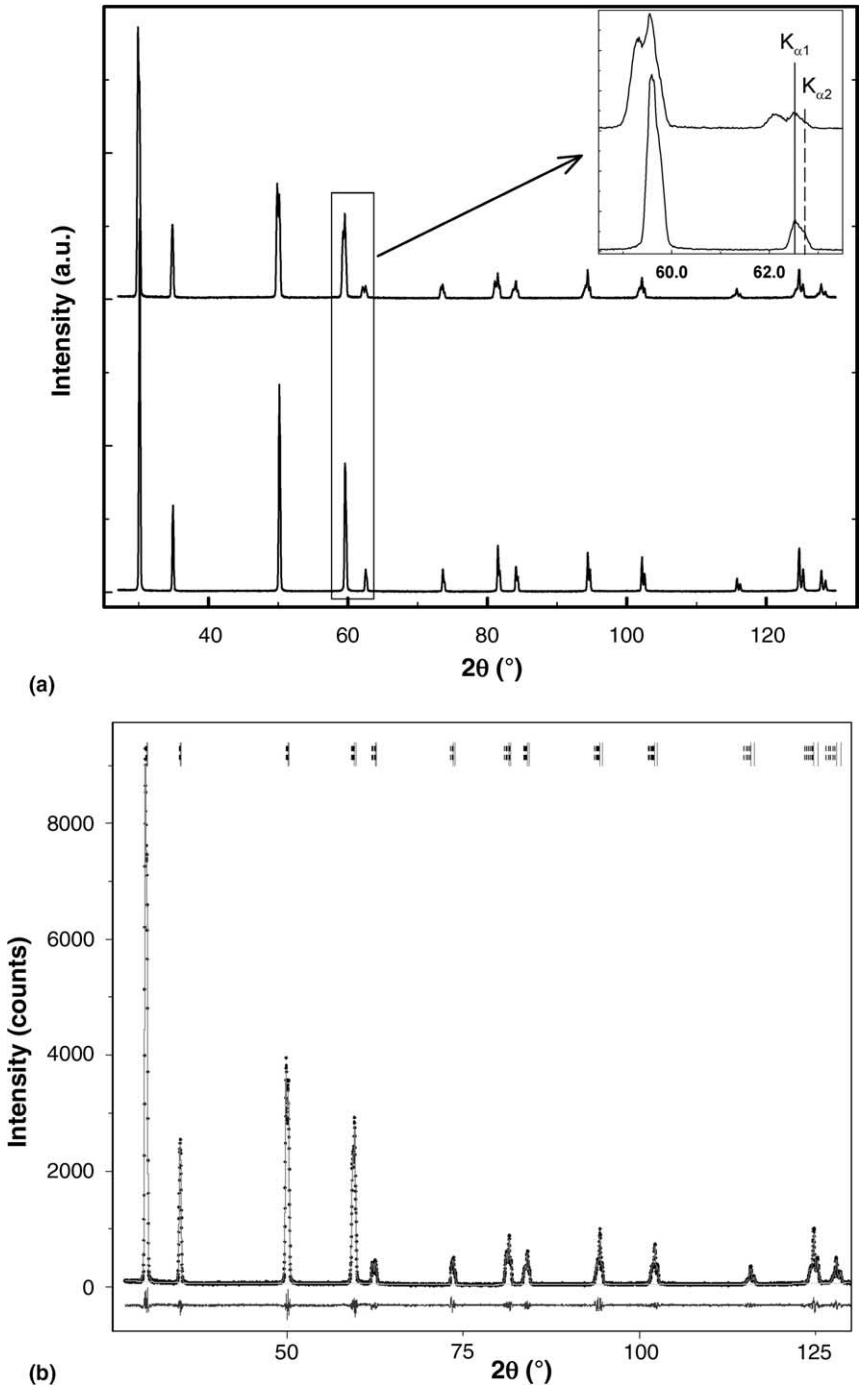

Fig. 1. (a) GXRD patterns recorded on CYSZ before and after He-implantation at 5×10^{16} cm^{-2}. The inset presents a zoom of the 58–64° region which exhibits both the $K_{\alpha 1}$, $K_{\alpha 2}$ doublet of the Cu K_{α} radiation, and a new diffraction line in the He-implanted sample. (b) Comparison between experimental GXRD pattern recorded on CYSZ after He-implantation at 5×10^{16} cm^{-2} (crosses) and calculated values (solid line) with a whole pattern LeBail fitting. The difference between both sets of data is shown in the lower part of the figure. Vertical marks indicate the positions of Bragg reflections for cubic (solid line) and rhombohedral (dashed line) phases.

A similar c → r transformation was previously observed by Hasegawa et al. [15] after N_2 ion implantation in zirconia. The same authors reported also the formation of a rhombohedral phase on the

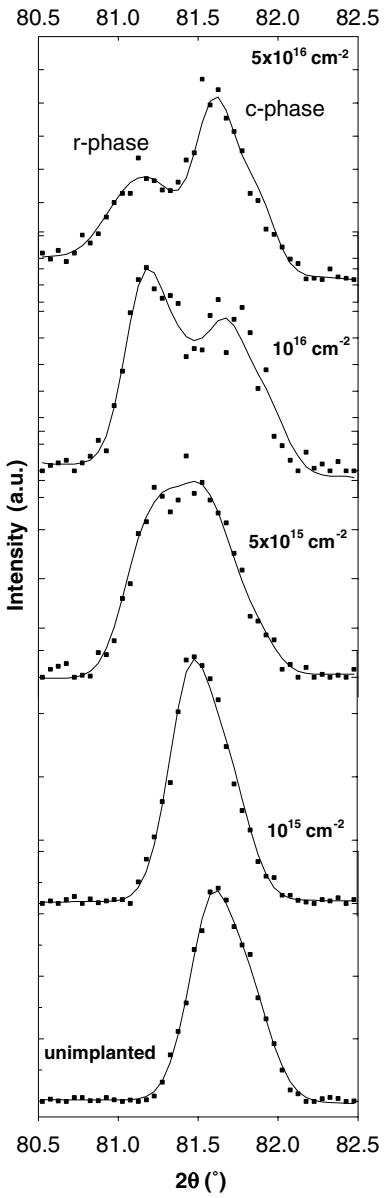

Fig. 2. Evolution with the He fluence of the c-(3 3 1) diffraction peak (cubic phase) and of the peak corresponding to the r-(3 2 2), r-(3 1 1) and r-(2 $\bar{1}$ 0) triplet of the rhombohedral phase.

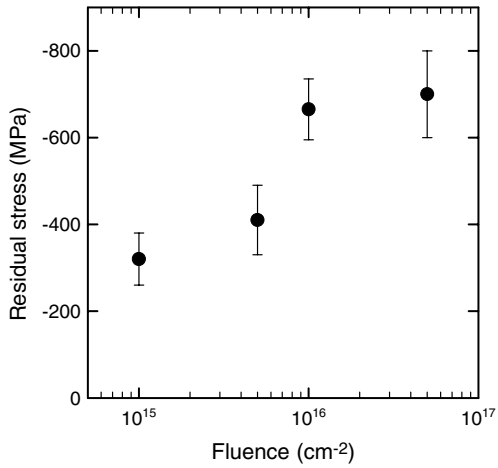

Fig. 3. Variation with the He fluence of the residual stress in the implanted layer of CYSZ.

abraded surface of fully-stabilized zirconia. On the other hand, Kondoh estimated, from aging treatments performed on fully and partially stabilized zirconia but without irradiation or implantation, that the existence of a rhombohedral phase in the ZrO_2–Y_2O_3 system is very doubtful [16]. He argued that the hump observed on the left shoulder of XRD peaks in yttria-stabilized zirconia is caused by a lattice distortion due to short-range ordering (SRO) of oxygen vacancies. However, the diffraction pattern associated with SRO vacancies is constituted of diffuse scattering with broadened and ill-defined peaks. In our experiments the new peaks are sharper than the large humps observed by Kondoh, so that they can be attributed to a c → r phase transformation induced by the large strain associated to He implantation.

Whether the introduction of He species or the creation of defects (by ballistic processes due to the nuclear energy loss of incident ions) contribute the most to the c → r phase transition evidenced by GXRD experiments is still an open question. In the former case the fraction of rhombohedral phase would depend on the concentration of implanted species (or on the concentration of He bubbles), whereas in the latter case this fraction would be related to the amount of radiation defects (i.e. to the number of displacements per atom of the target (dpa) induced by irradiation). The first hypothesis seems to be more likely in the light of recent channeling results which demonstrate that the transition from a low to a high degree of disorder in stabilized zirconia implanted with noble-gas ions is triggered by the defect formation for heavy elements (Ar, Kr, Xe) and by implanted species for light elements (He) [17]. Further experiments with heavy noble-gas ions are in progress to check this dilemma. The effect of the implantation temperature will also be examined to investigate the influence of the gas-bubble formation on the c → r phase transition.

4. Conclusion

Grazing-incidence X-ray diffraction experiments on cubic yttria-stabilized zirconia polycrystalline samples show that He ion implantation induces a cubic-to-rhombohedral phase transformation. This phase transition consists in a rhombohedral deformation of the cubic cell along the $\langle 1\,1\,1\rangle$ directions associated with residual stresses created in the implanted layer. The origin of the stresses is either the introduction of a given concentration of He atoms (which may form bubbles) or radiation defects produce by implantation.

Acknowledgements

The authors are grateful to O. Kaitasov for assistance during ion implantation and to N. Dragoe for help during the analyses with the GSAS package. This scientific program was partially supported by the GDR NOMADE.

References

[1] W.L. Gong, W. Lutze, R.C. Ewing, J. Nucl. Mater. 277 (2000) 239.
[2] E.H. Kisi, C.J. Howard, Key Eng. Mater. 153&154 (1998) 1.
[3] E.C. Subaro, Zirconia an overview, in: A.H. Heuer, L.W. Hobbs (Eds.), Science and Technology of Zirconia, Advances in Ceramics, The American Ceramic Society, Columbus, OH, 1981, p. 1.
[4] D. Simeone, J.L. Bechade, D. Gosset, A. Chevarier, P. Daniel, H. Hillaire, G. Baldinozzi, J. Nucl. Mater. 281 (2000) 171.
[5] D. Simeone, D. Gosset, J.L. Bechade, A. Chevarier, J. Nucl. Mater. 300 (2002) 27.
[6] A. Benyagoub, F. Levesque, F. Couvreur, C. Gibert-Mougel, C. Dufour, E. Paumier, Appl. Phys. Lett. 77 (2000) 3197.
[7] A. Benyagoub, Nucl. Instrum. and Meth. B 206 (2003) 132.
[8] J.A. Valdez, M. Tang, Z. Chi, M.I. Peters, K.E. Sickafus, Nucl. Instrum. and Meth. B 218 (2004) 103.
[9] K.E. Sickafus, H. Matzke, T. Hartmann, K. Yasuda, J.A. Valdez, P. Chodak III, M. Nastasi, R.A. Verrall, J. Nucl. Mater. 274 (1999) 66.
[10] D. Simeone, G. Baldinozzi, D. Gosset, S. LeCaër, L. Mazerolles, Phys. Rev. B 70 (2004) 134116.
[11] J.F. Ziegler, J.P. Biersack, U. Littmark, The Stopping and Range of Ions in Solids, Pergamon, New York, 1985.
[12] I.C. Noyan, J.B. Cohen, Residual Stress, Measurement by diffraction and Interpretation, Springer-Verlag, New York, 1987.
[13] N. Dragoe, J. Appl. Crystallogr. 34 (2001) 535.
[14] A.C. Larson, R.B. Von Dreele, General structure analysis system, LANSCE, Los Alamos National Laboratory, Report LAUR 86–748, 2000.
[15] H. Hasegawa, T. Hioki, O. Kamigaito, J. Mater. Sci. Lett. 4 (1985) 1092.
[16] J. Kondoh, J. Alloys Compd. 375 (2004) 270.
[17] L. Thomé, J. Fradin, J. Jagielski, A. Gentils, S.E. Enescu, F. Garrido, Eur. Phys. J. Appl. Phys. 24 (2003) 37.